22nd International Conference on Renewable Energies and Power Quality (ICREPQ'24)
Bilbao (Spain), 26th to 28th June 2024
Renewable Energy and Power Quality Journal (RE&PQJ)
ISSN 2172-038 X, Volume No.22, September 2024

Peak Current Mode Control for Grid-Connected Energy Storage Inverters

László Stranyóczky, András Futó, Szabolcs Veréb, István Varjasi and Zoltán Sütő

Department of Automation and Applied Informatics
Faculty of Electrical Engineering and Informatics
Budapest University of Technology and Economics
Műegyetem rkp. 3., H-1111 Budapest, Hungary

Abstract. Nowadays, three-phase inverters are playing an increasingly important role in various applications, such as drives, solar systems, energy storage systems. The commonly used PI current control method in the d-q coordinate system satisfies the requirements of most of the cases. However, in some specific applications, such as a grid-connected inverter for an energy storage system, the PI controller response time may not be sufficient to meet the criteria. This paper describes the application of the PCMC (Peak Current Mode Control) control technique, which is commonly used for DC-DC converters, and applies it to the case of three-phase two-level inverters. Advantages and disadvantages of PCMC compared to a conventional PI control solution are presented, and the performance of the two control techniques is compared for a grid connected energy storage inverter.

Key words. Inverter, Grid, Peak Current Mode Control, PCMC, Energy storage system, Simulation, Simulink

1. Introduction

The growing environmental awareness has led to an increasing adoption of household solar systems connected to the grid. However, the variable energy output from these systems poses challenges, necessitating the implementation of energy storage solutions to maintain grid stability. To tackle this issue, integrating battery packs via grid-connected inverters emerges as a straightforward and effective strategy for enhancing grid performance. These inverters manage the flow of energy between the grid and storage, ensuring stability during fluctuations and bridging gaps when solar generation fails.

Beyond the existing control demands for the inverter's power regulation, grid-connected inverters have to meet high standards. These requirements include the management of voltage fluctuations within the grid and the handling of possible short circuits. Taking these requirements into account, the block diagram shown in Figure 1 has been created, which shows the energy storage system with battery packs and the grid-connected inverter. The inverter receives its input DC voltage from a high-voltage (720 V) battery pack through a DC filter and a disconnection switch. The output voltages are directly connected to the phase inductances and then wired back to the midpoint of the DC link midpoint through capacitors. This design effectively helps meet EMC standards by reducing high-frequency noise. The AC output of the inverter passes through an AC filter and an AC switch, which allows the disconnection from the grid when necessary [1].

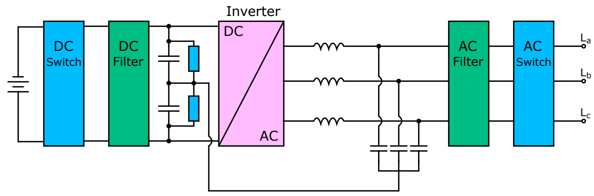

Fig. 1. The block diagram of the grid-connected energy storage system

In case of three-phase grid-connected inverters, a commonly used control method involves using PI current regulators within the d-q coordinate system. In this setup, the currents aligned with the d and q directions correspond to the active and reactive components of the grid's current. Thus, this arrangement allows for straightforward control of both active and reactive power on the grid. However, when dealing with energy storage inverters, an additional requirement arises: these inverters must not shut down with overcurrent faults caused by short circuits or voltage drops on the grid. Achieving this criterion is challenging, even with a well-tuned PI controller. If the regulator fails to respond immediately to such events, unintended high current diagnostics may be triggered, leading to the activation of the inverter's protection functions and shutdown [2].

One promising approach could be the utilization of Peak Current Mode Control (PCMC), commonly used in DC-DC converters. By applying PCMC to a grid-connected three-phase inverter within energy storage systems, these high requirements could be efficiently handled. To be specific, with carefully tuned slope compensation, the PCMC controller achieves a fast response (within a single switching period) to possible voltage drops on the grid. Furthermore, grid-connected inverters may resonate with other unidentified grid elements, but this resonance can also be avoided by using PCMC control [3][4].

2. Peak Current Mode Control

The Peak Current Mode Control (PCMC) is an improved version of the two-point regulator whose significant advantage lies in its ability to rapidly achieve the desired current value by providing the highest possible voltage. However, the two-point regulator has drawbacks due to its variable switching frequency. To address these limitations, the Peak Current Mode Control (PCMC) was developed. PCMC maintains a constant switching frequency, resulting in improved performance [5].

PCMC also introduces a damping effect at high frequencies. This occurs because an increase in current leads to a reduction in duty ratio, resulting in a decrease in the average output voltage of the inverter. The actual simulated resistance value, which is influenced by various factors, is positive. The upper frequency limit for resistance emulation is determined not by the converter's switching frequency but by the delays introduced by the control loop. This loop includes components such as the analog current sensor, analog comparator, digital logic, gate drive electronics, and switching transistor delay.

Implementing PCMC for three-phase inverters presents challenges due to the complex waveforms. In typical 3-phase, 2-level inverters with a floating star point on the AC side capacitor bank, each phase current waveform has four breakpoints per period. These breakpoints occur because of the high-frequency voltage between the capacitor bank's star point and the DC-link. However, in topologies where the AC side capacitor bank star point is connected to the DC link, the four breakpoints in the current waveform can be reduced to two. As a result, the phase current waveforms take on a triangular shape, and their high-frequency components become independent from each other. The drawback of this approach is that it requires large capacitors, which drives up equipment costs. However, for our specific scenario involving only a few units for the energy storage systems, it remains feasible due to its straightforward implementation [6][7].

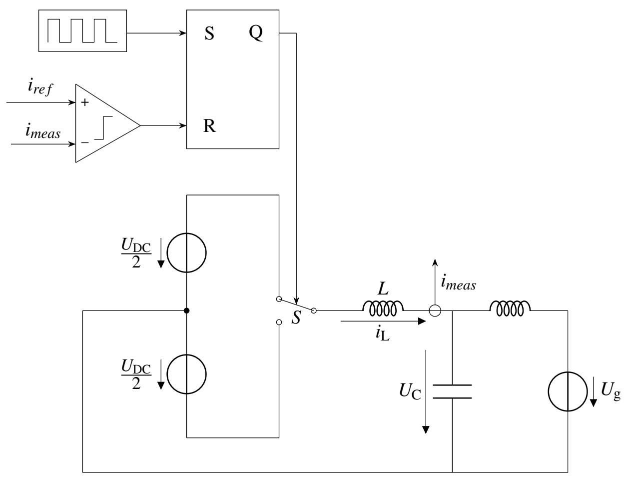

Fig. 2. Simplified circuit of the system

At the core of PCMC implementation, there is an RS flip-flop with a fixed-period pulse signal at its set input. When the pulse is triggered, the flip-flop output sets the two-position switch (S) to $\frac{U_{DC}}{2}$, applying a positive voltage to the output. As a result, i_L inductance current increases until the measured current (i_{meas}) reaches the reference (i_{ref}). The comparator output then enters a logic high state, causing the RS flip-flop to switch the two-position switch to $-\frac{U_{DC}}{2}$, leading to a decrease in current until the next pulse is received from the oscillator. This cyclic process repeats periodically [8]. Figure 2 shows the simplified circuit of the system for one phase, where the inverter is considered as an ideal two-position switch [9][10].

A. Slope compensation

Peak Current-Mode Control (PCMC) remains stable without any adjustments as long as the output voltage (U_C) remains below half of the DC link voltage (U_{DC}). To expand the stability range in terms of voltage, slope compensation is usually applied. The fundamental idea behind slope compensation is to gradually decrease the reference current linearly from the start of each switching period [11]. This concept is illustrated in Figure 3 with yellow.

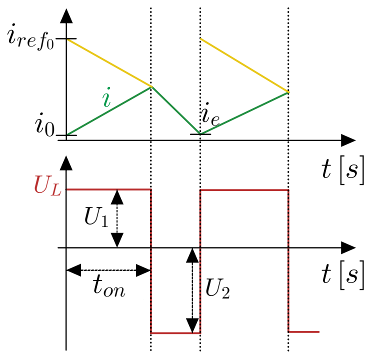

Fig. 3. Output voltage and current levels of slope compensated PCMC

Slope compensation not only extends the operating range but also has the advantage of significantly reducing the controller's response time. When properly adjusted, the controller can react in as short time as one switching period [12] [13]. Referring to Figure 2 and Figure 3, the output voltage values correspond to the two switch positions are $U_1 = \frac{U_{DC}}{2} - U_C$ and $U_2 = -\frac{U_{DC}}{2} - U_C$. The correct slope compensation requires adjustments to both the initial value and the slope itself. The initial value (i_{ref_0}) can be expressed using the following equation:

$$i_{ref_0} - i_0 = t_{on}\left(-\frac{di_{ref}}{dt} + \frac{di}{dt}\right), \tag{1}$$

where $\frac{di}{dt} = \frac{U_1}{L}$ and $\frac{di_{ref}}{dt}$ is the slope.

From this, the value of the current at the end of the switching period (i_e) can be determined by the formula

$$i_e = \hat{i} + \frac{U_2}{L}\, t_{off} = i_{ref_0} + \frac{di_{ref}}{dt}\, t_{on} + \frac{U_2}{L}\,(T - t_{on}), \tag{2}$$

where the peak current is

$$\hat{i} = i_{ref_0} + \frac{di_{ref}}{dt}\, t_{on}. \tag{3}$$

By rearranging Equation (2) and substituting Equation (3), i_e can be expressed in a form (Equation (4)) where it is clear that i_e becomes independent of i_0 when the appropriate slope is chosen. This implies that the value of the current at the end of the switching period is independent of the value at the beginning of the switching period, which is the end of the previous switching.

$$i_e = i_{ref_0}\left(1+\frac{\frac{di_{ref}}{dt}-\frac{U_2}{L}}{-\frac{di_{ref}}{dt}+\frac{U_1}{L}}\right)+\frac{U_2}{L}T-\frac{\frac{di_{ref}}{dt}-\frac{U_2}{L}}{-\frac{di_{ref}}{dt}+\frac{U_1}{L}}i_0. \tag{4}$$

The correct slope value for the independence of i_0, in which case the response of the controller can be as fast as only one switching period, can be calculated from the following equation:

$$\frac{di_{ref}}{dt}=\frac{U_2}{L}=\left(-\frac{U_{DC}}{2}-U_C\right)\frac{1}{L}, \tag{5}$$

so the slope of the reference current is equal to the slope of the current in the off state.

3. Simulation

To validate the functionality of the PCMC for a three-phase, two-level grid-connected inverter, a system plant model and control scheme was created using MATLAB Simulink. The system model includes components such as the DC bus (representing the battery pack), the inverter model, and the grid model with the grid filter. Within this model, grid voltage fluctuations can easily be simulated to test the response time of the PCMC control.

In the control subsystem, both the described PCMC current control structure and a more general PI control solution was implemented in parallel. To facilitate comparison, the reference inputs for both controllers are derived from $i_{d_{ref}}$ and $i_{q_{ref}}$ reference current values, which are transformed back into phase values for the PCMC version.

A. PCMC

In the PCMC implementation discussed in Section 2., a fixed-period pulse signal is connected to the set input of the RS flip-flop. However, in this scenario, the resulting PWM signals are not center-aligned. Therefore, this implementation is not utilized in the simulation. Instead, a PWM signal is generated conventionally using a triangular carrier signal with third harmonic injection modulation. This resulting PWM signal serves as the turn-off signal for the PCMC. The turn-on event is triggered by the sign change of the difference between the measured current and the reference current. The achieved final PWM signal is center-aligned.

In the simulation, slope compensation is applied as described in Section 2.A. While at simulation level, knowing the grid parameters, both the inductance of the system and the compensation slope can be accurately determined. However, in reality, this determination relies on measurements. By realizing multiple measurements on the current within a switching period, its slope can be calculated, enabling the determination of the inductance value for the optimal slope value, that ensures the fastest possible controller response time. Figure 4 shows the simulation results using the PCMC controller and Table I contains the simulation parameters.

$f_{grid} = 50\ Hz$
$f_{switching} = 6\ kHz$
$U_{DC} = 650\ V$
$I_{d_{ref}} = 220\ A$
$I_{q_{ref}} = 50\ A$
$L_{grid} = 40.41\ \mu H$
$\hat{U}_{grid} = 230 \cdot \sqrt{2}\ V$

Table I. Parameters of the PCMC simulation

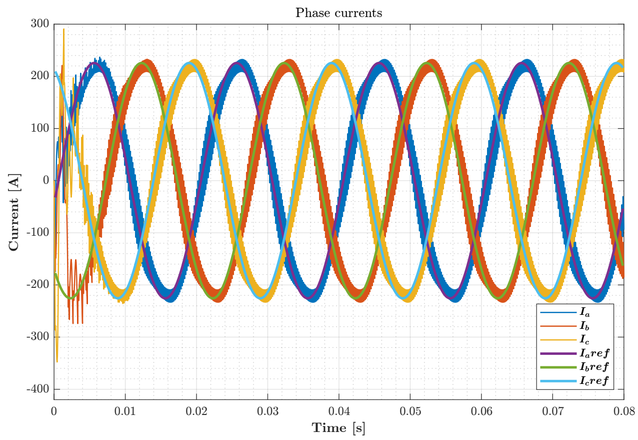

Fig. 4. Measured and reference phase current results of the PCMC simulation

Figure 5 shows the reference current, the slope-compensated reference current and the measured current in a zoomed view. It can be clearly seen that the slope of the compensation equals to the slope of the measured current in the off state.

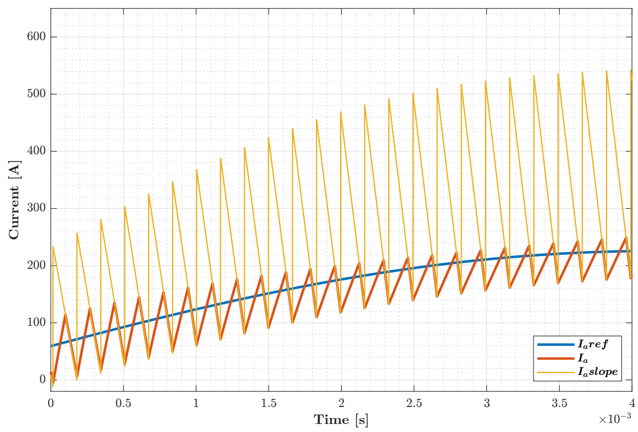

Fig. 5. Measured, reference and compensated reference phase current of the PCMC simulation

B. PI Current Control

The more general controller, designed within the d-q coordinate system, uses a digital PI current controller for both the I_d and I_q currents. The tuning and implementation of the digital control loop followed the procedure described in [14]. To achieve a control response with a small overshoot, a phase margin of 60 degrees was chosen, with the remaining phase distributed between the loop delay and the PI controller in a 2/3 and 1/3 ratio.

The controller outputs are U_d and U_q voltages, which are then transformed back into phase values. A third harmonic injection is applied to this transformed three-phase voltage system, ensuring the maximum $\frac{U_{DC}}{\sqrt{3}}$ voltage output of the inverter. By dividing this modulated voltage by the DC voltage, we get duty cycles, which can be used to easily generate PWM signals using a triangle carrier.

Connecting the AC side capacitor bank star point to the DC link allows zero-order current to flow through the inverter, so relying only on simple d and q direction current control is not sufficient for stability, as the first chart of Figure 6 also shows. To suppress this, a virtual zero-sequence resistor ($R_0 = 0.3\ \Omega$) is introduced into the regulator. The calculated voltage from the measured zero-sequence current and R_0 is subtracted from the reference voltages of the PWM modulators, along with third harmonic injection. As a result, the system achieves stability, and the phase currents follow the reference currents, as demonstrated in the lower chart of Figure 6. The simulation of the implemented controller uses the parameters outlined in Table I.

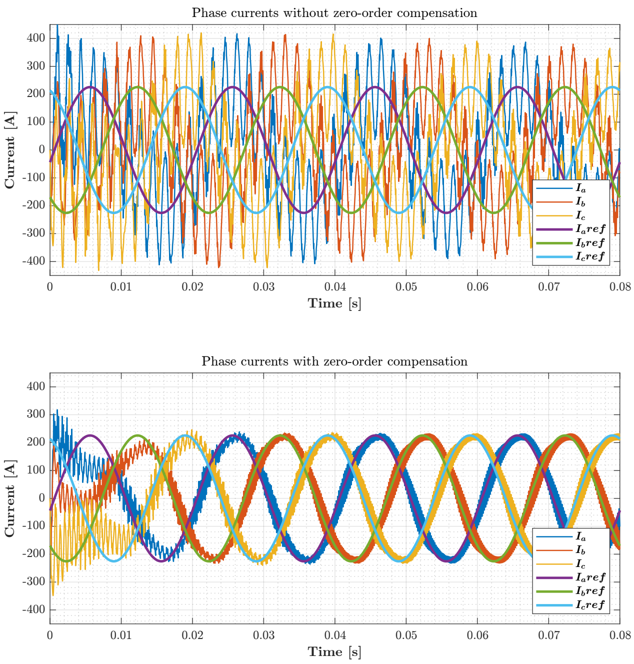

Fig. 6. Phase currents with PI controller without and with zero-order resistance.

In case of the PI current controller, it can be seen that the initial transients in the simulation settle more slowly than in the PCMC case.

C. Comparison

Both controllers operate with switching frequency (6 kHz). They are triggered precisely at the lower peaks of the carrier triangle signal, which correspond to the current measurement. This timing is crucial because it allows sampling of the current at the middle of its ripple, ensuring regulation to the desired average value. That is why the creation of center-aligned PWM signals for PCMC was essential. Additionally, the controller outputs are initially stored in a shadow register, simulating the behaviour of a real microprocessor.

After verifying that both controllers operate optimally under ideal conditions, the next step is to test how quickly they react to potential grid voltage fluctuations. To evaluate this test, the peak voltage value of the grid model was multiplied by a modifying signal. This signal jumps from 1 to 0.7 in 1 ms, simulating a 30 % voltage drop.

As demonstrated in the previous section, the PI controller version reacts significantly slower to transient events. As shown in Figure 7, the current approximately doubles from the original peak value of 225.6 A because of the applied 30 % voltage drop on the grid. In contrast, the PCMC controller solution shows a more moderate increase of approximately 40 A under the same circumstances. The difference between the two methods can also be seen in the d-q transformed currents (Figure 8).

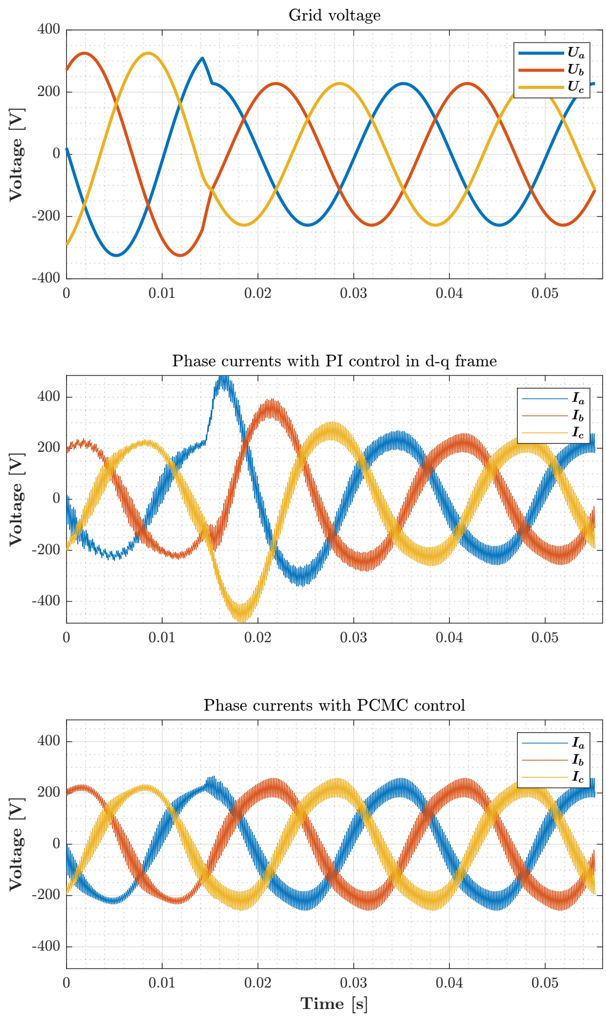

Fig. 7. Response of the two control approach to 30 % grid voltage drop

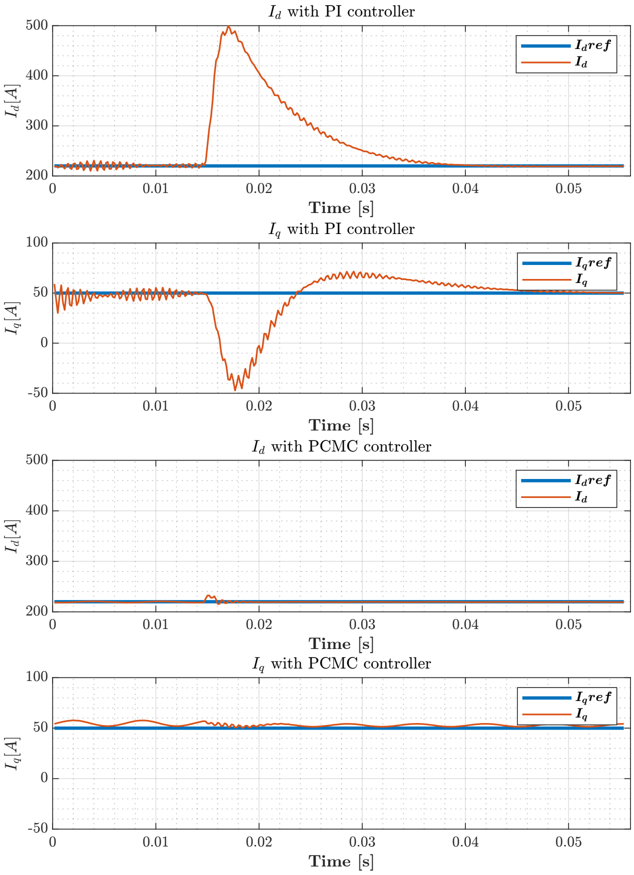

Fig. 8. Response of the two control approach to 30 % grid voltage drop

This current difference may affect the operation of a grid-connected inverter in an energy storage system, as it may be the case that the inverter controlled by the PCMC does not turn off due to an overcurrent fault, while the more general PI controlled inverter does. Note, that the studied PI controller does not contain feed-forward component with the capacitor voltage. Applying feed-forward term can speed up the PI control behaviour, but at the same time it could increase the chance of instability due to additional harmonics at the grid side.

4. Conclusions

This paper explores the utilization of PCMC (Peak Current Mode Control) in case of three-phase two-level grid-connected inverters. While this controller is typically associated with DC-DC converters, it also finds relevance in special inverter applications, such as the discussed energy storage system . Its implementation costs extra, since it requires large capacitors through which the AC output is connected to the DC link. This design ensures compliance with EMC conditions. Despite its implementation cost, the PCMC controller becomes essential in certain situations where the more common PI regulator inverter might disconnect from the grid due to grid voltage fluctuations. Furthermore, the use of PCMC acts as a damping resistor at high frequencies, thus preventing other unknown elements in the network from causing resonance.

Acknowledgments

Supported by the ÚNKP-23-3-I-BME-27 New National Excellence Program of the Ministry for Culture and Innovation from the source of the National Research, Development and Innovation Fund.

References

[1] K.-B. Park and S. Pettersson, “Peak current control for three-phase inverter with lcl filter.” IEEE, 5 2021, pp. 104–107.

[2] W. Choi, W. Lee, and B. Sarlioglu, “Effect of grid inductance on grid current quality of parallel grid-connected inverter system with output lcl filter and closed-loop control.” IEEE, 3 2016, pp. 2679–2686.

[3] J. Munoz-Cruzado-Alba, J. Villegas-Nunez, J. A. Vite-Frias, E. Galvan-Diez, and J. Carrasco, “A new fast peak current controller for transient voltage faults for power converters.” IEEE, 6 2015, pp. 166–171.

[4] B. Baby and K. Mathew, “Modified peak and valley current mode control of single phase full bridge voltage source inverter using flux cancellation method.” IEEE, 12 2023, pp. 261–267.

[5] D. G. Holmes, R. Davoodnezhad, and B. P. McGrath, “An improved three-phase variable-band hysteresis current regulator,” *IEEE Transactions on Power Electronics*, vol. 28, pp. 441–450, 1 2013.

[6] N. Kobayashi, Y. Hayashi, S. Iyasu, and Y. Handa, “Digital peak current mode control method for the single-phase bi-directional dc-ac converter.” IEEE, 9 2021, pp. P.1–P.8.

[7] ——, “Fast current control of the single-phase dc-ac converter using digital peak current mode control.” IEEE, 9 2019, pp. P.1–P.7.

[8] M. Aime, G. Gateau, and T. Meynard, “Implementation of a peak current control algorithm within a field programmable gate array.” IEEE, 2004, pp. 941–946 vol. 2.

[9] M. Ebrahimi and S. A. Khajehoddin, “Fixed-frequency generalized peak current control (gpcc) for inverters.” IEEE, 3 2016, pp. 3207–3212.

[10] K. S. Prakash and M. Barai, “Time-variant slope compensation for peak current mode control (pcmc) of boost converter with point-of-load applications.” IEEE, 3 2016, pp. 1–6.

[11] S. Amir, R. van der Zee, and B. Nauta, “An improved modeling and analysis technique for peak current-mode control-based boost converters,” *IEEE Transactions on Power Electronics*, vol. 30, pp. 5309–5317, 9 2015.

[12] M. S. Manoharan, A. Ahmed, and J.-H. Park, “Digital implementation of peak current mode control for single-phase h-bridge inverter with slope compensation.” IEEE, 10 2013, pp. 1502–1506.

[13] F. Tian, S. Kasemsan, and I. Batarseh, “An adaptive slope compensation for the single-stage inverter with peak current-mode control,” *IEEE Transactions on Power Electronics*, vol. 26, pp. 2857–2862, 10 2011.

[14] S. Veréb, A. Futó, Z. Süttö, A. Balogh, and I. Varjasi, “Continuous cross-period single phase shift control for dual active bridge converters,” *Renewable Energy and Power Quality Journal*, vol. 19, pp. 222–228, 9 2021.